Nathaniel Beall Bunnell

Department of Biochemistry

Phosphate Ester Bond Chemistry with Zirconium (IV) Catalysts

Thesis Defense Date: Thursday, March 31st

Committee Members:

Robert Kuchta, Department of Biochemistry – Thesis Advisor
Jeffrey Cameron, Department of Biochemistry
Kurtis Hessel, Program for Writing and Rhetoric

Abstract

Earth's infancy was a time of immense chemical complexity. Over many millions of years, steady chemical cycles were formed and driven by thermodynamics and organic precursors left over from the planet's formation. In aqueous environments, this chemistry may have led to the formation of catalytic RNA species capable of information storage and replication. Presumably, the formation of these oligonucleotides was catalyzed by primordial Earth's abundant mineral content. However, the species that accelerated these types of transformations are unknown. In this study, the role of Zr^{+4} in the catalytic formation of phosphate ester bonds was explored. Through TLC screening, it was found that most of the test conditions produced no observable phosphorylated products. In the final samples, there were highly polar spots which may have contained phosphate-bearing compounds. These findings provide mixed certainty about zirconium's catalytic capacity for ester formation but suggest that zirconium metal organic frameworks (MOFs) and alternative metal ions may be viable routes for future investigation.

Introduction

The origin of life is one of the most elusive mysteries present within the biological or chemical disciplines. While an immense amount of knowledge about modern metabolisms, enzyme mechanisms, and cellular structures has been collated, we only have a limited understanding of the first biological processes that took place on Earth.

It is broadly assumed that the initial step in Earth's transition to an organismal planet involved the genesis of simple chemical systems that mimicked the fundamental metabolisms seen today. For example, in porous rock located within Earth's primordial oceans, chemical reactions involving small organic reagents may have occurred via the assistance of exposed minerals or simply via thermodynamic favorability. If these processes were recursive (circular), they could stably produce increasing amounts of organic product (Trefil et al. 2009). In turn, this reliable chemical output would allow for the creation of increasingly complex chemical compounds via downstream reactions (Figure 1). Over vast swaths of time, an ancient, thermodynamically driven Earth would shape basic metabolic pathways and form complex organic molecules with properties advantageous to the earliest forms of life (Trefil et al. 2009).

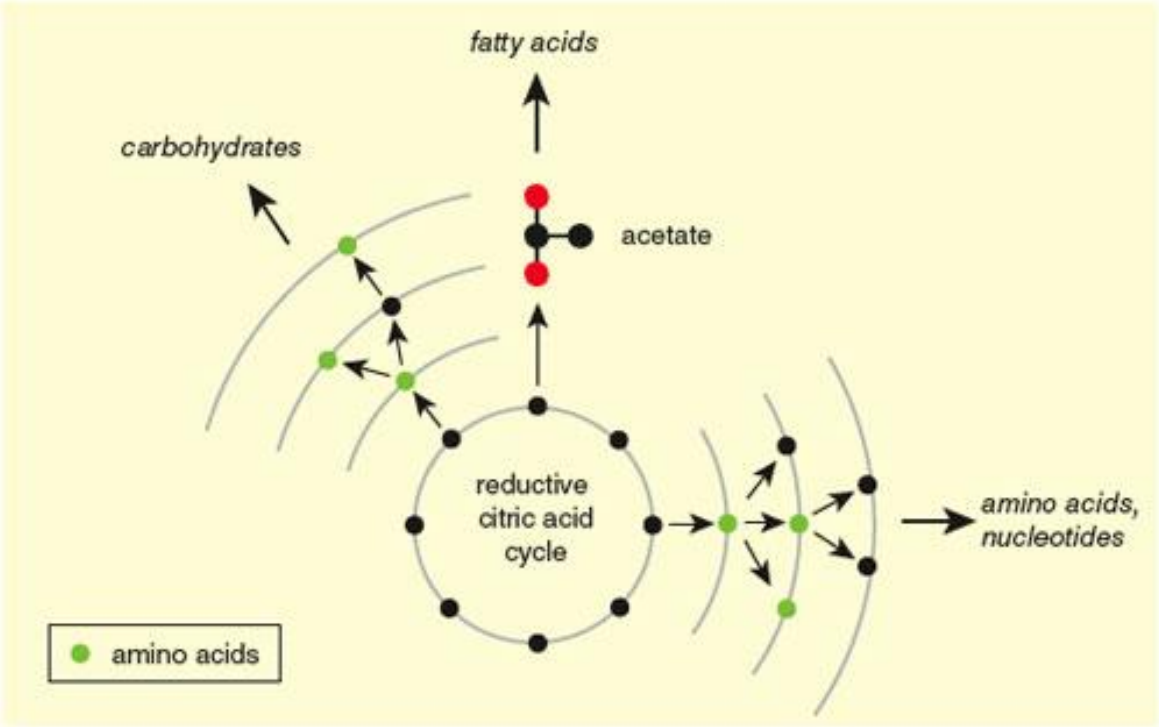

Figure 1: Simple Metabolic Pathways Can Create Complex Biological Precursors. The first chemical transformations resembling the metabolisms seen in organisms today likely involved simple, repetitive cycles of incoming reagent and outgoing product. Assuming a steady supply of reagent, these cycles would eventually generate enough product for more complex chemistry to occur. In this image, the reductive version of the citric acid cycle pulls electrons and energy from inorganic sources and uses these reservoirs to synthesize organic compounds from CO_2. The surrounding layers symbolize the number of times the cycle must be run before the molecules on the arc can form (innermost arc requires two runs of the cycle, while the next furthest arc requires three). Through the cascade of additional syntheses resulting from the products of this one cycle, all the key building blocks of biological molecules can be formed. *Image courtesy of Trefil et al. 2009.*

A crucial step in Earth's metabolic progression is the leap from small carbon products to structures capable of true catalysis and replication. While key intermediary details of this jump are unknown, the broad strokes are summarized in the "RNA World" hypothesis. In this theory, the convergence of basic metabolisms and thermodynamic energy requirements resulted in the synthesis of limited RNA or RNA-like fragments that were able to be replicated via their organized, 4-base template structure (Alberts et al. 2002). Work by Thomas Cech and Sidney Altman in the 1980s demonstrated that RNA molecules can act as enzyme-like catalysts, with their model system being capable of self-cleavage (Trefil et al. 2009). This finding suggests that early RNA sequences may have been capable of self-replication, thus satisfying the principles of information storage and growth that all modern organisms rely on. The many possible conformational states of RNA and their affinity for metal ions, behaviors characteristic of modern enzymes, further support this inference.

If RNA systems developed polymerase capability, natural selection would inevitably follow. As strands of RNA were copied, occasional errors would result in the production of novel sequences. The survival and propagation of these mutants would depend on their structural stability and their utility to the original RNA system. If they conferred a "survival" advantage to the proto-polymerase RNA, like the catalytic synthesis of ribonucleotides, they would be more likely to be preserved via polymerization by said ribozyme. In this way, groups of cooperative RNA strands may have formed under primordial conditions, with each sequence performing specialized roles critical to the group's longevity (Alberts et al. 2002).

An evident shortcoming of this model is the consideration of proximity. Namely, how were RNA molecules able to remain isolated in their cooperative system (without a boundary, sequences might migrate between systems and cause intersystem competition), and how was the system able to keep all the requisite sequences close enough to continue operating? A potential solution may be amphipathic molecules. Amphipathic molecules contain distinct hydrophobic and hydrophilic groups within their overall structure. This divide encourages these molecules to assemble in structures that have water-facing polar groups and aggregated nonpolar groups. When phospholipids, a type of amphipathic molecule, are suspended in water, they spontaneously form circular vesicles that expose their hydrophilic heads to aqueous solution while isolating their lipophilic tails inside the vesicle. If a similar aggregative process occurred near a cooperative RNA system, the strands may have become trapped in a vesicular structure that resembled modern cellular membranes (Alberts et al. 2002). Now, the development of this cooperative system was dependent on more than just the fitness of its RNA partners, but also on the RNA's interactions with the surrounding molecules and entrapping membrane. Through a chance engulfment, a replicating RNA system would become intertwined with the fate of a lipid membrane and would become a primitive version of today's complex cellular life.

Upon isolation in the membrane, natural selection within the proto-cell environment likely produced the biological hallmarks of protein synthesis and DNA formation. Production of mutant RNAs may have eventually created sequences with high affinity for certain amino acids. Previous RNA selection research has shown evidence of this process, with the high affinity sequences often having a disproportionately large frequency of the codon for the amino acid that they bind to (Alberts et al. 2002). With the help of ribozymes that aminoacylate at semi-catalytic speeds, these primitive tRNAs may have led to a system of templated protein synthesis that mirrors the system seen today. Similar evolutionary factors could have led to mutant RNAs that were able to produce deoxyribose from ribose or other carbon precursors. Eventually, this may have escalated into the production of DNA, a far more stable genetic material owing to its resistance to hydrolysis. The evolutionary behavior of RNA can feasibly produce almost all other aspects of modern life, an observation that lends much credit to the RNA world hypothesis.

Unfortunately, the crucial assumption of the RNA hypothesis is ironically the aspect most shrouded in mystery. Before it could lead to higher forms of life, *how* was RNA formed in the first place? RNA synthesis is an energetically costly procedure, due to the placement of negatively charged phosphate groups near one another. In today's cells, this process is aided by energy yielded from the hydrolysis of the di or triphosphate forms of the nucleotides being added (LibreTexts, 2014). During primordial times, these complex species were presumably rare or nonexistent, meaning the synthesis of RNA would have been facilitated by other energy sources

or catalytic species. To better understand life's origins, it is crucial to identify simple oligonucleotide synthesis schemes that can feasibly fill the gaps of this ancient chemical history.

Because ancient water sources were filled with mineral-rich rock from extraterrestrial debris (Lunine 2006), transition and lanthanide metal ions show great promise as new subjects of study via their tendency to accelerate the hydrolysis of oligo species. As free ions or part of a heterogeneous hydroxide gel, Ce (IV) ions have been shown to increase oligonucleotide hydrolysis rates by more than a million-fold, presumably due to activation of the phosphate backbone via their high charge to size ratio (Ott and Krämer 1998). Similarly, cobalt complexes have been observed to increase the rate of hydrolysis of the DNA backbone by factors of 10^6 to 10^8 (Sreedhara and Cowan 2001).

Traditional catalysts increase the rate of a reaction by lowering the activation energy, E_a, of said reaction (Libretexts 2022). However, this accelerates the forward and reverse reactions equally, since in theory all chemical reactions are fully reversible (Libretexts 2022). By this logic, the use of catalytic metal complexes under favorable conditions might incentivize the formation of phosphomonoester or phosphodiester bonds, the reverse process of the hydrolysis described above.

In this thesis, the role of zirconium (IV) ions in the catalytic formation of oligonucleotide species was examined. Zirconium was selected because of its lengthy history of hydrolytic reactions with nucleic acid-like species. The earliest investigations of this metal indicated that it was capable of hydrolysis of the phosphodiester bond of bis(*p*-nitrophenyl) phosphate at rates more than 10^8 times faster than spontaneous hydrolysis at pH 7 and 25 ^oC (Ott and Krämer 1998). Cleavage rates at varying $ZrCl_4$ concentrations exhibited Michaelis-Menten like behavior when plotted against 1 / v in Lineweaver Burk Plots (Ott and Krämer 1998, Figure 2). Zr^{+4} has also shown phosphate hydrolysis behavior in complexes containing EDTA, Tris, and 2,6-pyridinedimethanol (Ott and Krämer 1999), in coordination with peptides containing serine terminus residues and histidine ligands (Berkessel and Herault 1999), and in complex metal organic frameworks containing Zr_6 nodal centers with coordinated Zinc ions (Zhou et al. 2019).

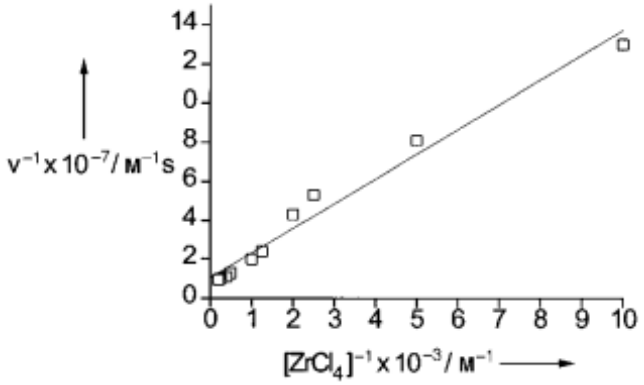

Figure 2: Lineweaver Burk Plot of $ZrCl_4$ Demonstrates Michaelis Menten Activity. Inversion of the Michaelis-Menten Equation produces data with a linear trend for catalysts or enzymes that behave in accordance with the Michaelis-Menten model. This behavior is observed

for the zirconium (IV) ion, with more than 80% of the variation in the dataset being accounted for by a line of best fit. From the plot, we can easily calculate the K_M to be 0.001 M. *Image courtesy of Ott and Krämer 1998.*

To assess the feasibility of phosphate bond formation via zirconium species, we investigated a variety of different experimental conditions suspected to encourage catalytic behavior. Resulting samples were screened for the presence of CMP or benzyl phosphate (compounds that indicate successful phosphate linkage) via thin layer chromatography (TLC), a simple technique that allows for the visualization of added compounds based on their relative polarity and chemical properties.

Materials and Methods

Sample Preparation

Numerous sampling conditions were trialed to determine zirconium's capacity for phosphate bond formation.

The generation 1 batch (G1) was composed of varying concentrations of $ZrCl_4$, cytidine nucleoside, monosodium phosphate, and Tris in saturated sodium chloride solution (Table 1).

Solution #	Final $ZrCl_4$ Concentration (M)	Final Cytidine Concentration (M)	Final NaH_2PO_4 Concentration (M)	Final Tris Concentration (M)
1	0.1	0.1	0.1	-
2	0.1	0.1	0.1	0.1
3	0.5	0.5	0.1	-
4	0.5	0.5	0.1	0.1
5	0.5	0.1	0.1	-
6	0.1	0.5	0.1	-

Table 1: Generation 1 Solutions. Requisite amounts of solid were weighed and added to 1.5 mL Eppendorf tubes without the use of stock solutions and suspended in an aqueous, saturated sodium chloride solution. All samples were added to a heating block and heated for a period ranging from 24 to 32 hours.

After preparation and testing of the generation 1 solutions, a new batch of solutions utilizing benzyl alcohol in place of cytidine was prepared in aqueous solution saturated with sodium chloride. These solutions are demonstrated in table 2.

Solution #	Final $ZrCl_4$ Concentration (M)	Final NaH_2PO_4 Concentration (M)	Volume of Benzyl Alcohol (µL)
1	0.2	0.1	100
2	0.5	0.1	100

C	-	0.1	100

Table 2: Generation 2 (G2) Solutions. Solid zirconium (IV) chloride and monosodium phosphate were weighed and added directly to 1.5 mL Eppendorf tubes until the desired concentrations were achieved. Benzyl alcohol and saturated sodium chloride solutions were added to each of the Eppendorf tubes until a total volume of 1 mL was achieved. All solutions were heated for 24-48 hours at 65 ^{o}C on a heating block after preparation.

After generation 2 was assayed, a third generation of solutions was prepared based on further insight into potentially favorable conditions and additional manipulable variables. Most notably, the generation three solutions included $MgCl_2$, were pH varied, and utilized a few different solvent combinations.

G3 Solution 1	**G3 Solution 2**	**G3 Solution 3**
50 µL $ZrCl_4$ (NaCl Stock) 100 µL Phosphate Buffer 100 µL $MgCl_2$ 50 µL Benzyl Alcohol 700 µL Aqueous Saturated NaCl Solution **pH = 3-4**	50 µL $ZrCl_4$ (NaCl Stock) 200 µL Phosphate Buffer 100 µL $MgCl_2$ 50 µL Benzyl Alcohol 600 µL Aqueous Saturated NaCl Solution **pH = 7**	50 µL $ZrCl_4$ (NaCl Stock) 225 µL Phosphate Buffer 100 µL $MgCl_2$ 50 µL Benzyl Alcohol 550 µL Aqueous Saturated NaCl Solution 25 µL NaOH Solution **pH = 9-10**
G3 Solution 4	**G3 Solution 5**	**G3 Solution 6**
50 µL $ZrCl_4$ (NaCl Stock) 100 µL Phosphate Buffer 100 µL $MgCl_2$ 50 µL Benzyl Alcohol 350 µL Aqueous Saturated NaCl Solution 350 µL Pure DMSO **pH = 3-4**	50 µL $ZrCl_4$ (NaCl Stock) 200 µL Phosphate Buffer 100 µL $MgCl_2$ 50 µL Benzyl Alcohol 300 µL Aqueous Saturated NaCl Solution 300 µL Pure DMSO **pH = 7**	50 µL $ZrCl_4$ (NaCl Stock) 225 µL Phosphate Buffer 100 µL $MgCl_2$ 50 µL Benzyl Alcohol 275 µL Aqueous Saturated NaCl Solution 275 µL Pure DMSO 25 µL NaOH Solution **pH = 9-10**
G3 Solution 7	**G3 Solution 8**	**G3 Solution 9**
50 µL $ZrCl_4$ (DI Water Stock) 100 µL Phosphate Buffer 100 µL $MgCl_2$ 50 µL Benzyl Alcohol 350 µL DI Water 350 µL Pure DMSO **pH = 3-4**	50 µL $ZrCl_4$ (DI Water Stock) 200 µL Phosphate Buffer 100 µL $MgCl_2$ 50 µL Benzyl Alcohol 300 µL DI Water 300 µL Pure DMSO **pH = 7**	50 µL $ZrCl_4$ (DI Water Stock) 225 µL Phosphate Buffer 100 µL $MgCl_2$ 50 µL Benzyl Alcohol 275 µL DI Water 275 µL Pure DMSO 25 µL NaOH Solution **pH = 9 - 10**

G3 Solution 10 (Benzyl Alcohol Control)	G3 Solution 11 (Benzyl Alcohol Control)	G3 Solution 12 (Benzyl Alcohol Control)
50 µL $ZrCl_4$ (NaCl Stock) 250 µL Phosphate Buffer 100 µL $MgCl_2$ 600 µL Aqueous Saturated NaCl Solution	50 µL $ZrCl_4$ (NaCl Stock) 250 µL Phosphate Buffer 100 µL $MgCl_2$ 300 µL Aqueous Saturated NaCl Solution 300 µL Pure DMSO	50 µL $ZrCl_4$ (DI Water Stock) 250 µL Phosphate Buffer 100 µL $MgCl_2$ 300 µL DI Water 300 µL Pure DMSO
pH = 7	**pH = 7**	**pH = 7**

Table 3: Generation 3 (G3) Zirconium Solutions. Stock solutions of 0.25 M $ZrCl_4$ were prepared in saturated sodium chloride solution and DI water. A phosphate buffer for the G3 solutions was prepared by dissolving monosodium phosphate into DI water until a concentration of 0.5 M was achieved. The buffer was adjusted to contain conjugate phosphate species via the addition of sodium hydroxide. $MgCl_2$ was added via a 0.1 M stock solution in DI water. Necessary pH adjustments were made via the addition of 1 M hydrochloric acid or 1 M sodium hydroxide until the desired pH range was measured by a color-changing pH strip. All the solutions were heated at 65-70 ^oC for approximately 192 hours.

Saturated urea solutions were prepared to test the effect of this species on the catalytic properties of zirconium (IV). These urea solutions examined the same parameters that were tested in the G3 solutions. Namely, the pH was varied to examine the effects of acidity and basicity on zirconium catalysis (Table 4).

U Solution 1	U Solution 2	U Solution 3	U Solution 4 (Benzyl Alcohol Control)
50 µL $ZrCl_4$ (Urea Stock) 100 µL Phosphate Buffer 100 µL $MgCl_2$ 100 µL Benzyl Alcohol 650 µL Saturated Urea Solution	50 µL $ZrCl_4$ (Urea Stock) 200 µL Phosphate Buffer 100 µL $MgCl_2$ 100 µL Benzyl Alcohol 550 µL Saturated Urea Solution	50 µL $ZrCl_4$ (Urea Stock) 225 µL Phosphate Buffer 100 µL $MgCl_2$ 100 µL Benzyl Alcohol 520 µL Saturated Urea Solution 5 µL NaOH Solution	50 µL $ZrCl_4$ (Urea Stock) 200 µL Phosphate Buffer 100 µL $MgCl_2$ 650 µL Saturated Urea Solution
pH = 3-4	**pH = 7**	**pH = 10**	**pH = 7.2**

Table 4: Urea (U) Zirconium Solutions. Urea solutions were prepared in 1.5 mL Eppendorf tubes via the addition of the reagents described above. $ZrCl_4$ was added via preparation of a 0.25 M solution of the compound in water saturated with urea. $MgCl_2$ was added via a 0.1 M stock in DI water. Necessary pH adjustments were made via the titration of each sample by 1 M hydrochloric acid or 1 M NaOH. After preparation, all samples were put on a heating block and kept at 65-70 ^oC for 192 hours.

After the urea and G3 batch trials, a new round of samples was composed and concentrated on a speed-vacuum apparatus to remove any aqueous solution. These samples were then reconstituted in benzyl alcohol and heated for approximately 4-5 days (96-120 hours, Table 5).

Dehydrated Solution 1	**Dehydrated Solution 2**	**Dehydrated Solution 3**
100 µL $ZrCl_4$ (NaCl Stock) 100 µL Phosphate Buffer 100 µL $MgCl_2$ 700 µL NaCl Solution 100 µL EDTA 50 µL $ZrCl_4$ (NaCl) Added for pH Adjustment **pH = 4.1**	100 µL $ZrCl_4$ (NaCl Stock) 200 µL Phosphate Buffer 100 µL $MgCl_2$ 600 µL NaCl Solution 200 µL EDTA **pH = 7**	100 µL $ZrCl_4$ (NaCl Stock) 225 µL Phosphate Buffer 100 µL $MgCl_2$ 550 µL NaCl Solution 25 µL NaOH 225 µL EDTA 7.5 µL NaOH Added for pH Adjustment **pH = 9-10**
Dehydrated Solution 4	**Dehydrated Solution 5**	**Dehydrated Solution 6**
100 µL $ZrCl_4$ (NaCl Stock) 100 µL Phosphate Buffer 100 µL $MgCl_2$ 350 µL NaCl Solution 350 µL Pure DMSO 100 µL EDTA 50 µL $ZrCl_4$ (NaCl) Added for pH Adjustment **pH = 4**	100 µL $ZrCl_4$ (NaCl Stock) 200 µL Phosphate Buffer 100 µL $MgCl_2$ 300 µL NaCl Solution 300 µL Pure DMSO 200 µL EDTA **pH = 7**	100 µL $ZrCl_4$ (NaCl Stock) 225 µL Phosphate Buffer 100 µL $MgCl_2$ 275 µL NaCl Solution 275 µL Pure DMSO 25 µL NaOH 225 µL EDTA 10 µL NaOH Added for pH Adjustment **pH = 9-10**
Dehydrated Solution 7	**Dehydrated Solution 8**	**Dehydrated Solution 9**
100 µL $ZrCl_4$ (DI Water Stock) 100 µL Phosphate Buffer 100 µL $MgCl_2$ 350 µL DI Water 350 µL Pure DMSO 100 µL EDTA 200 µL $ZrCl_4$ (DI) Added for pH Adjustment	100 µL $ZrCl_4$ (DI Water Stock) 200 µL Phosphate Buffer 100 µL $MgCl_2$ 300 µL DI Water 300 µL Pure DMSO 200 µL EDTA	100 µL $ZrCl_4$ (DI Water Stock) 225 µL Phosphate Buffer 100 µL $MgCl_2$ 275 µL DI Water 275 µL Pure DMSO 25 µL NaOH 225 µL EDTA 50 µL NaOH Added for pH Adjustment

pH = 4-5	pH = 7	pH = 10
Dehydrated Solution 10 (Phosphate Control) 100 µL $ZrCl_4$ (NaCl Stock) 100 µL $MgCl_2$ 800 µL NaCl Solution 200 µL EDTA 110 µL NaOH Added for pH Adjustment **pH = 7**	**Dehydrated Solution 11 (Phosphate Control)** 100 µL $ZrCl_4$ (NaCl Stock) 100 µL $MgCl_2$ 400 µL NaCl Solution 400 µL DMSO 200 µL EDTA 110 µL NaOH Added for pH Adjustment **pH = 7**	**Dehydrated Solution 12 (Phosphate Control)** 100 µL $ZrCl_4$ (DI Water Stock) 100 µL $MgCl_2$ 400 µL DI Water 400 µL DMSO 200 µL EDTA 110 µL NaOH Added for pH Adjustment **pH = 7**
Dehydrated Solution 13 (Zirconium (IV) Chloride Control) 500 µL Phosphate Buffer 100 µL $MgCl_2$ 400 µL NaCl Solution 200 µL EDTA **pH = 7**	**Dehydrated Solution 14 (Zirconium (IV) Chloride Control)** 500 µL Phosphate Buffer 100 µL $MgCl_2$ 200 µL NaCl Solution 200 µL DMSO 200 µL EDTA **pH = 7**	**Dehydrated Solution 15 (Zirconium (IV) Chloride Control)** 500 µL Phosphate Buffer 100 µL $MgCl_2$ 200 µL DI Water 200 µL DMSO 200 µL EDTA **pH = 7**

Table 5: Dehydrated Zirconium Solutions. Dehydrated solutions were initially prepared in the requisite solvents and concentrated under vacuum. Zirconium (IV) chloride was added to each sample via the addition of liquid volumes from NaCl and DI water stock solutions. Phosphate buffer was added via a 0.5 M stock of monosodium phosphate prepared in DI water and modified by NaOH for increased buffering capacity. $MgCl_2$ was added via a 0.1 M stock prepared in DI water. After the first concentration, EDTA was added to each solution to prevent the formation of zirconium phosphate species (via isolation of zirconium ions in metal organic frameworks, or MOFs). Each sample was concentrated after the addition of this ligand. Necessary pH adjustments were performed before the first and second concentrations via the addition of 0.25 M $ZrCl_4$ solution or 1 M NaOH solution. Fully concentrated samples were reconstituted in pure benzyl alcohol and heated at 65 ^oC for 5 days.

The concentration methodology was also applied to a batch of zirconium samples containing saturated urea solution, as seen in the following table.

DU Solution 1	DU Solution 2	DU Solution 3	DU Solution 4 (Phosphate Control)	DU Solution 5 (Zirconium (IV) Chloride Control)
100 µL $ZrCl_4$ (Urea Stock) 100 µL	100 µL $ZrCl_4$ (Urea Stock) 200 µL	100 µL $ZrCl_4$ (Urea Stock) 225 µL	100 µL $ZrCl_4$	

Phosphate Buffer 100 µL $MgCl_2$ 700 µL Saturated Urea Solution 100 µL EDTA 200 µL $ZrCl_4$ Added for pH Adjustment **pH = 3-4**	Phosphate Buffer 100 µL $MgCl_2$ 600 µL Saturated Urea Solution 200 µL EDTA 20 µL NaOH Added for pH Adjustment **pH = 7.8**	Phosphate Buffer 100 µL $MgCl_2$ 550 µL Saturated Urea Solution 25 µL NaOH 225 µL EDTA 52.5 µL NaOH Added for pH Adjustment **pH = 10-11**	(Urea Stock) 100 µL $MgCl_2$ 800 µL Saturated Urea Solution 200 µL EDTA 110 µL NaOH Added for pH Adjustment **pH = 7-8**	500 µL Phosphate Buffer 100 µL $MgCl_2$ 500 µL Saturated Urea Solution 200 µL EDTA **pH = 7-8**

Table 6: Dehydrated Urea (DU) Zirconium Solutions. Dehydrated samples were prepared in aqueous solution saturated with urea and later concentrated under vacuum. Zirconium (IV) chloride was added to each sample via a 0.25 M urea stock solution. Phosphate buffer was prepared by dissolving 0.5 M of monosodium phosphate into DI water and modifying its buffer capacity via the addition of sodium hydroxide. $MgCl_2$ was added via a 0.1 M stock prepared in DI water. After the first concentration step, EDTA was added to each solution to prevent the formation of zirconium phosphate species. Each sample was concentrated after the addition of this ligand. Necessary pH adjustments were performed before the first and second concentrations via the addition of 0.25 M $ZrCl_4$ solution or 1 M NaOH solution. Fully concentrated samples were reconstituted in benzyl alcohol and heated at 65-70 ^oC for 4 to 5 days.

The final round of prepared solutions included Tris and EDTA, two compounds known to form metal complexes with zirconium ions. These samples were similarly dehydrated and reconstituted in benzyl alcohol before heating.

TE Solution 1	**TE Solution 2**	**TE Solution 3**	**TE Solution 4 (Phosphate Control)**	**TE Solution 5 (Zirconium (IV) Chloride Control)**
400 µL $ZrCl_4$ (DI Water Stock) 100 µL Tris 500 µL Phosphate Buffer 100 µL $MgCl_2$ 100 µL EDTA 100 µL $ZrCl_4$ Added for pH Adjustment **pH = 4-5**	400 µL $ZrCl_4$ (DI Water Stock) 100 µL Tris 500 µL Phosphate Buffer 100 µL $MgCl_2$ 100 µL EDTA 10 µL NaOH Added for pH Adjustment **pH = 7**	400 µL $ZrCl_4$ (DI Water Stock) 100 µL Tris 500 µL Phosphate Buffer 100 µL $MgCl_2$ 100 µL EDTA 25 µL NaOH Added for pH Adjustment **pH = 10**	400 µL $ZrCl_4$ (DI Water Stock) 100 µL Tris 100 µL $MgCl_2$ 100 µL EDTA 500 µL of NaOH Added for pH Adjustment **pH = 8-9**	100 µL Tris 500 µL Phosphate Buffer 100 µL $MgCl_2$ 100 µL EDTA **pH = 7**

Table 7: Tris-EDTA (TE) Zirconium Solutions. Samples were prepared in solution and later concentrated under vacuum. Zirconium chloride was added to each sample from a 0.25 M stock in DI water. Tris and EDTA stock solutions were mixed with added zirconium chloride and

incubated for 30 minutes to an hour before the addition of phosphate. Phosphate buffer was prepared by creating a monosodium phosphate – DI water mixture with a 0.5 M concentration. This stock was then converted into a dual species buffer via the addition of 1 M sodium hydroxide. $MgCl_2$ was added from a 0.25 M stock in DI water. Necessary pH adjustments were performed by the addition of aqueous $ZrCl_4$ or NaOH. Completed samples were concentrated under vacuum for 12 hours, resuspended in benzyl alcohol, and heated for 4-5 days at 65-70 ^oC.

Thin Layer Chromatography

Thin Layer Chromatography, or TLC, is an affinity method used to separate compounds based on their relative polarities (Sigma-Aldrich 2022). In this technique, solid phase silica is used to cover a metal (typically aluminum) plate. This plate is then spotted with the samples of interest at an origin line (which is typically drawn towards the bottom of the plate) and placed in a developing chamber containing some sort of solvent medium. As the liquid medium moves up the plate by capillary action, different components of the spotted sample will move different distances based on their preferred affinity for the solvent or the solid medium (Sigma-Aldrich 2022). Generally, polar compounds will interact more favorably with the solid plate, and thus will move less far than their non-polar counterparts. This means that higher spots are often produced by compounds that are comparatively less polar than other species located on the plate.

Once the solvent line lies a few millimeters below the top of the plate, the plate is pulled out of the TLC chamber and a line is drawn at the final distance of the solvent's movement. The R_f value, which is given by the distance traveled by the component spot divided by the distance traveled by the solvent front, is often calculated after the plate has been developed. To visualize components of the spotted sample mixture, UV or iodine stains are often used (CHEM CU Boulder 2022).

The generation 1 (G1) solutions were developed on solid silica gel plates in TLC chambers with 90% water and 10% methanol solvent systems. The plates were run for 5-10 minutes and were marked under a UV lamp.

The generation 2 (G2) solutions were developed under similar conditions, excepting the use of 1:1 hexanes and ethyl acetate in place of the solvent system described above. Later runs of the G2 solutions made use of solvent systems containing different percentages of water and methanol.

The generation 3 solutions were run at different time points during the reaction (0, 24, 48, 72, and 192 hours). Each sample was run in a pure water solvent system and a separate pure ethyl acetate solvent system. The resulting plates were allowed to dry and were visualized with a UV lamp.

The dehydrated solutions, dehydrated urea solutions (DU), and Tris-EDTA (TE) solutions were also run at different time points during the reaction, but at longer intervals than the generation 3 solutions (0, 120 hours) due to time considerations. All samples were screened using a solvent system composed of 1:1 ethanol and ethyl acetate and a pure ethyl acetate system and visualized with UV light.

Results

Investigation of the role of Zr^{+4} in the catalytic formation of phosphoester bonds began with the generation 1 (G1) solutions, which contained varying concentrations of $ZrCl_4$, sodium monobasic phosphate, cytidine, and Tris. These samples were prepared in aqueous solution containing saturating concentrations of sodium chloride to reduce the water activity of these samples. Because water is a product of phosphomonoester synthesis, isolation of this species via high salt concentrations shifts the reaction equilibrium towards the product side by Le Chatelier's principle. Additionally, high salt concentrations reduce the likelihood of water forming stabilizing hydration shells around polar reactants like monobasic phosphate, further encouraging these species to react.

TLC assays of the G1 samples revealed spots produced by both nonpolar and polar compounds. For solutions 1 and 2, 3 separate components were identifiable after visualization with UV light. Upon comparison with an aqueous cytidine standard, one of these spots (in each solution) was attributed to the individual nucleoside, since the R_f values for the central spot of each of these samples matched perfectly with the R_f value for the cytidine control. However, the identity of the other spots remains unclear. For both solutions, one of the distinguishable spots lies above the cytidine standard, which indicates that the compound producing this spot is less polar than the cytidine nucleoside (Figure 3). However, the spot below the cytidine standard has greater polarity since it travelled a smaller distance along the TLC plate (Figure 3). This finding is significant since we would expect CMP species to be more polar than their non-phosphorylated counterparts. While this spot does lie at a decent height above the starting line, this is to be expected with the high polarity of the solvent system used. Generally, more polar solvent systems can compete for binding sites on the solid surface of the TLC plate more effectively (LibreTexts 2013). This results in all spotted material moving further up the solid phase plate, a phenomenon that would explain the distance covered by this unknown compound (LibreTexts 2013).

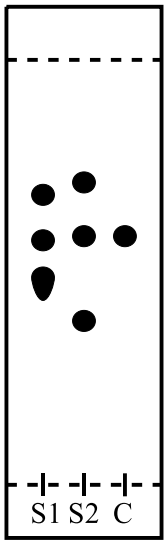

Figure 3: Generation 1 Solutions Contain Polar Compounds. A plate containing solutions 1 and 2 of generation 1 was run in a 90% water and 10% methanol solvent system. The plate was dried and visualized under a UV lamp. This work up revealed the presence of numerous spots in the lanes containing solutions 1 (S1) and 2 (S2). The central spots, which had R_f values of 0.58 and 0.59, were attributed to cytidine nucleoside, with the cytidine control (C) having a R_f value of 0.58. The nonpolar spots in lanes 1 and 2 had R_f values of 0.68 and 0.72, respectively. The polar spots located near the origin may have contained CMP or other phosphorylated derivatives. The polar spot in lane 1 had an R_f of 0.48 while its counterpart in lane 2 had an R_f of 0.37.

With the first trial producing encouraging results, a second generation of solutions (G2) was produced that substituted benzyl alcohol for the cytidine that was previously used. This switch was driven by reagent availability and the higher concentrations of benzyl alcohol that are achievable in solution. Because of structural similarities between the two reagents, including their aromatic rings and alcohol functionalities, it was assumed that they should have similar chemical reactivities.

Screening of the heated G2 samples in various solvent systems revealed a few spots with interesting placements. In the 1:1 hexanes and ethyl acetate solvent system, it was found that G2 solution 1 contained an additional spot when compared to the G2 control. This spot was higher on the TLC plate than the matching spots for the G2 control and solution 1, indicating that it was less polar than the pure benzyl alcohol (R_f = 0.85 compared to an R_f of 0.65 for benzyl alcohol). Because benzyl phosphate is much more polar than benzyl alcohol, this spot is presumably due to contamination or the formation of byproduct by the zirconium in solution. With the use of more polar solvent systems, including pure methanol and varying ratios of water and methanol, compound spots were identified within G2 solution 2. On these polar plates, both solution 1 and solution 2 had nearly identical compound distributions. Namely, each solution produced a nonpolar spot toward the top of the TLC plate and a significantly smaller, highly polar spot near the origin (Figure 4). Initially, it was postulated that these polar spots may have contained benzyl phosphate. While this is still a possibility, later observations lend credence to the argument that these polar spots are simply observable byproducts.

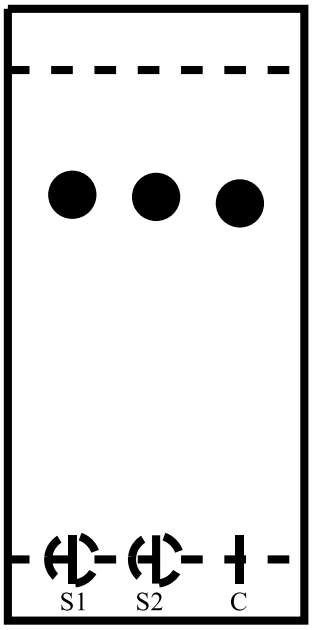

Figure 4: Generation 2 Solutions Contain Polar Spots at the Plate Origin. A plate containing G2 solution 1, 2, and the G2 zirconium control was run in a solvent system containing 75% water and 25% methanol. Upon visualization with a UV lamp, it was found that solutions 1 and 2 both contained a nonpolar spot towards the top of the plate and a polar spot (of less intensity, as indicated by the dashed circumference) at the origin line. Upon comparison with the control sample, the nonpolar spots seen in both G2 solutions can be attributed to unreacted benzyl alcohol, due to the similarity in their R_f values with the spot seen in the control. The polar spots may have been produced by small amounts of benzyl phosphate or by salt or other byproducts.

Generation 3 marked a turning point in the complexity of this thesis, primarily through the examination of pH effects and metal ion inclusions. For example, $MgCl_2$ was used to release Mg^{2+} ions into solution, since magnesium is a known cofactor for phosphodiester bond formation during DNA synthesis (Yang et al. 2004). The pH variations were implemented due to previous studies finding substantially different rates of hydrolysis based on changes in the sample pH (Ott and Krämer 1998). Finally, the differing solvent combinations were used to try and increase the solubility of some of the solid compounds being included in the samples.

The G3 samples were also assayed by TLC at a variety of different time points. As the concentration of product in the heated samples increased, any product spots on the TLC plates would show a darker color over time as more product was spotted per run.

Unfortunately, the G3 solutions demonstrated minimal change over time. In the pure ethyl acetate TLC system, solutions 1, 2, 3, and 10 demonstrated essentially no changes over 192 hours at 65-70 ^{o}C. On each plate, distinct spots were located at the starting line of each sample. These polar spots were also seen in the control sample (G3 S10), indicating that the compound being observed was a reagent, byproduct, or salt shared between all the samples (Figure 5). At

the top of the ethyl acetate plates, the first batch of G3 solutions demonstrated dark spots at all the different time intervals that were tested. However, upon comparison with a pure BA standard, it can be concluded that these spots are due to unreacted benzyl alcohol located within each sample, since they have R_f values that are nearly identical to each run standard (Figure 5). Much like the previous samples, S7, S8, S9, and S12 all had moderately polar spots that were seen during all time points. Comparison of R_f values attributed all these spots to pure benzyl alcohol (Figure 5). Additionally, highly polar spots were observed in all samples during the tested time points. Because these spots were in the S12 control sample, which lacked benzyl alcohol, it is extremely unlikely that they contain benzyl phosphate or any desirable phosphate derivative.

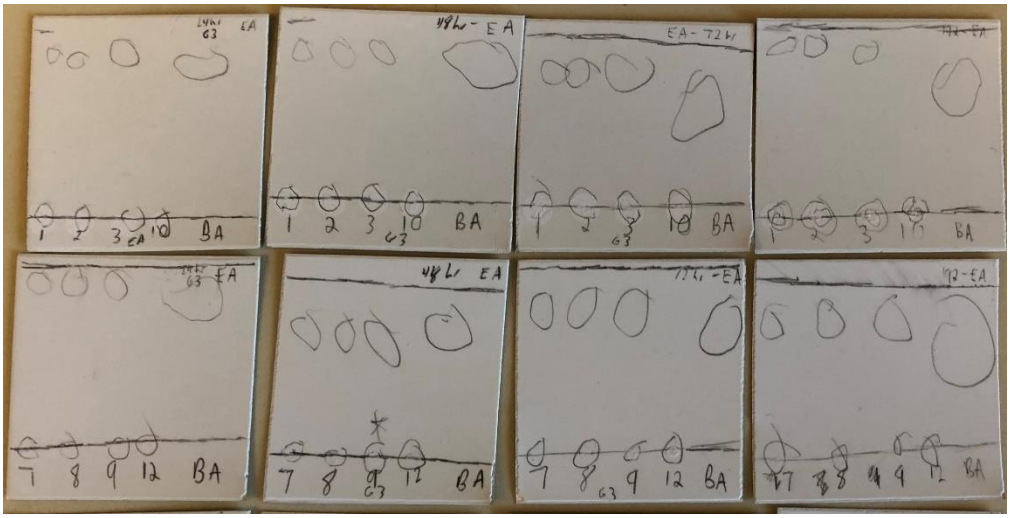

Figure 5: Generation 3 Plates Show No Change During the Timed Assays. Silica gel TLC plates containing G3 S1, S2, S3, and S10 or G3 S7, S8, S9, and S12, were run in solvent systems containing pure ethyl acetate or pure water (only the ethyl acetate plates are shown). Visualization under UV demonstrated that neither sample series had significant compositional changes during the 8-day testing period. On each plate, nonpolar spots near the solvent front correspond to unreacted benzyl alcohol. On the origin, almost every plate has dark, immobile polar spots that are seen in the experimental and control samples. Based on this overlap, these spots likely correspond to some type of common reactant or salt left over from spotting of the saturated samples.

TLC plates containing G3 S4, S5, S6, and S11 differed from their counterparts via the observation of highly polar streaks at the final time point (Figure 6). However, it is highly unlikely that these spots represent phosphate ester bond formation since the streak is also located in the control lane of S11. This control lacked benzyl alcohol, and thus would not have been able to form a benzyl phosphate product unless contamination occurred.

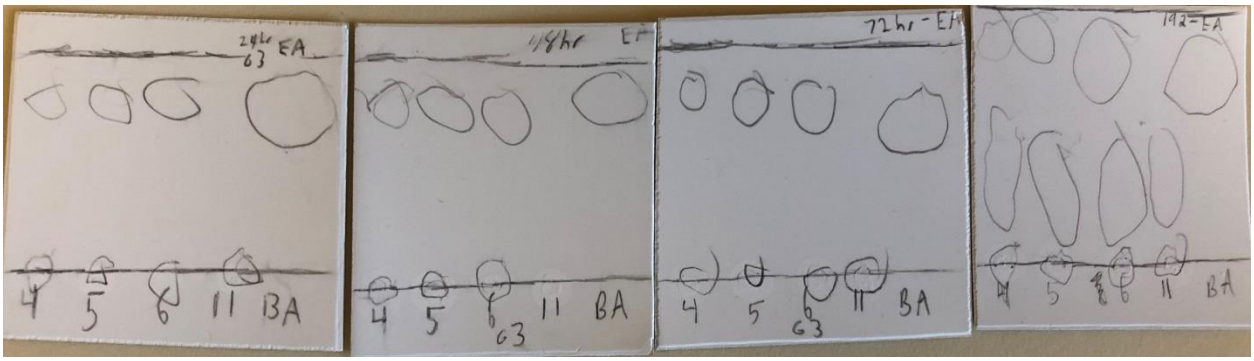

Figure 6: Generation 3 Solutions Demonstrate Polar Streaks at 192 Hours. TLC plates containing G3 S4, S5, S6, and S11 were run at 24, 48, 72, and 192 hours (as shown from left to right). Visualization under UV showed minimal changes from 0 to 72 hours. On the 192-hour plate, highly polar streaks can be seen in all the experimental lanes. Because of the presence of a polar streak in lane 11, this finding is likely due to contamination of the control or the formation of a polar byproduct during the heating process.

During the heating cycles of the G3 solutions, saturated urea solutions were prepared that were similarly tested at different pH values. Urea was tested due to theories of this species being present in concentrated pools on primordial Earth (Salván et al. 2020). Additionally, urea saturation performs a similar function to sodium chloride saturation. Namely, it binds free water molecules with incredibly high affinity due to its polar structure. In turn, the reaction mixture should be devoid of free water, which encourages ester bond formation via Le Chatelier's principle and the disruption of energetically favorable hydration shells.

Unfortunately, work-up of the urea solutions provided no evidence of benzyl phosphate formation. Across the 4 different time points, no spots of significant polarity were observed that were not seen within the control samples. Of the spots that were seen exclusively in the experimental samples, all were attributable to benzyl alcohol, due to similarity in the R_f values of these spots and plated benzyl alcohol standards.

The final rounds of prepared samples were dehydrated on a speed-vacuum concentrator to remove all remaining water. This eliminated hydration of the reactants and maximally shifted the phosphate reaction towards bond formation via Le Chatelier's principle. In the traditional samples (samples 1-15) minimal TLC changes were observed over a viewing interval of 120 hours, or five days. Each sample lane retained the relatively nonpolar spots corresponding to benzyl alcohol over the weeklong period. While these spots were large in magnitude, this was to be expected based on the reconstitution of these samples' solids in pure benzyl alcohol solution (Figure 7). Like many previous samples, the dehydrated samples contained highly polar spots located at the origin of each TLC plate. However, these spots were shared between the experimental samples and the controls, and thus are not attributable to desired compounds like benzyl phosphate. The dehydrated urea samples similarly provided no useful information (Figure 7).

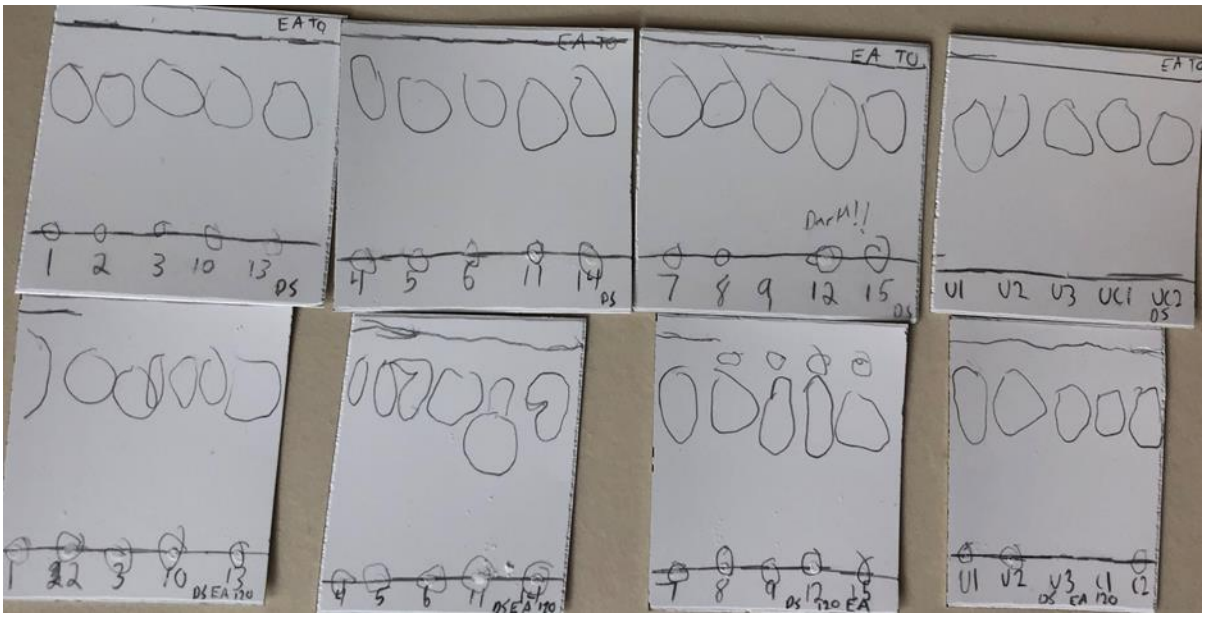

Figure 7: Conventional Dehydrated and Dehydrated Urea Samples Show No Changes Over 120 Hour Period. TLC plates containing dehydrated samples 1-15 and DU 1-5 were run in pure ethyl acetate and 1:1 ethyl acetate and ethanol solvent systems at 0 and 120 hours (only the ethyl acetate results are shown). Visualization with UV demonstrated consistent benzyl alcohol spots in all the assayed samples across time. After 120 hours, dehydrated solutions 8, 9, 12, and 15 all contained nonpolar spots above their respective benzyl alcohol spots. These spots are presumably due to byproduct formation during the extended heating period.

Of the dehydrated samples, the TE solutions had the most relevant results due to the presence of unidentifiable, polar spots within two of the sample lanes and two of the controls on the 120-hour TLC plate (Figure 8). These spots had R_f values of 0.15 – 0.17, well above the origin. Excepting the presence of the polar spots in the control lanes, this plate almost perfectly encompassed the qualitative results expected of a zirconium system that catalyzes phosphate bond formation. The presence of the polar spots in the control lanes may be attributable to contamination.

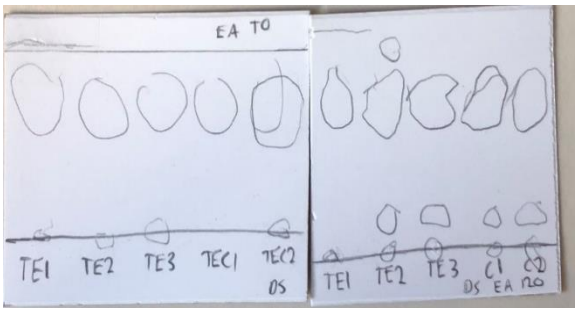

Figure 8: TE Samples Contain Highly Polar Spots Indicative of Phosphoester Formation. Dehydrated and heated TE samples were screened at 0 and 120 hours by TLC in an ethyl acetate solvent system and a 1:1 ethyl acetate and ethanol solvent system (only the ethyl acetate plates are shown). The resulting 120-hour plate contains 4 highly polar spots with R_f values ranging

from 0.15 to 0.17. These spots are in the lanes corresponding to TE 2, TE 3, TE 4 (phosphate control), and TE 5 (zirconium control).

Discussion

In generation 1, the presence of polar, unidentifiable spots provides mixed certainty about zirconium's ability to catalyze the formation of phosphomonoester or phosphodiester bonds. While small amounts of CMP may have formed under the tested conditions, other explanations are just as feasible. For example, zirconium is known to bind to phosphate in a ratio of 1 Zr^{4+} : 2 HPO_4^{2-} with high affinity and thermodynamic stability at room temperature (Awual et al. 2011). This compound is also incredibly polar and would be expected to travel in a similar fashion to CMP or CpC chains on a TLC plate based on this polarity overlap. Another issue of importance for the G1 solutions is how long the solutions were heated. The *hydrolysis* of DNA via zirconium species is a slow process, with k_{cat} values ranging from 4.9×10^{-3} to 2.9×10^{-7} s^{-1} at room temperature (Ott and Krämer 1998, 1999). Presumably, any bond formation processes involving phosphate would occur on the same kinetic time scale. Without extended heating, the reaction may not be accelerated to a degree where products would be visible. This issue was addressed in the later samples, but in the future, it might be fruitful to rerun the G1 samples with a heating time that stretches across days or weeks. Assuming polar spots form in this repeated run, they could be compared to dissolved standards of assumed contaminants like zirconium phosphate and subjected to mass spectrometry for accurate product identification.

The generation 2 solutions were similarly mediocre since the observed polar spots are more than likely caused by salt or some other common reagent. While these spots were not observed in the control lane of this generation, spots of similar magnitude and shape were seen in almost every G3 solution, including many of the controls. Additionally, the lack of movement of these spots, even in the presence of extremely polar water solvent systems, indicates that these spots are likely produced by some sort of contaminant or TLC issue instead of by a real product or soluble compound. Upon closer examination, many of the dark, polar spots in the G2 solutions were filled with a thin layer of crystalline material that was probably residual sodium chloride. Thus, the presence of these spots may be due to the blockage of the fluorescent silica by a thin layer of spotted salt instead of any desirable organic compound. During the initial runs of generation 2, a saturated salt standard was spotted alongside each of the experimental samples to account for the visual background of high salt concentrations. While this standard was phased out in later runs because of the increased number of parameters and reagents, it may be valuable to reintroduce such standards in future experimental runs that contain saturating concentrations of salt.

Regarding the G3 and urea solutions, numerous chemical factors likely contributed to the stagnancy of these solutions. As mentioned above, it is highly likely that some amount of zirconium phosphate formed during the mixing of the phosphate buffer and $ZrCl_4$. Throughout the runtime of the G3 solutions, white precipitate was visible at the bottom of many of the Eppendorf samples. Zirconium phosphate is quite insoluble in aqueous solutions, so this white solid may have been crude zirconium phosphate. This would have sequestered many of the functional zirconium ions, preventing them from acting as catalytic species (Hevesy and Kimura

1925). Upon encountering water, $ZrCl_4$ can also react to form zirconyl chloride or zirconium hydroxide (although zirconium hydroxide generally only forms at higher pH values). While these reactions are potentially minimized in the heavily saturated aqueous solutions, the G3 solutions lacking salt may have converted a portion of the added $ZrCl_4$ into these alternative species. In turn, these new compounds may have had reduced catalytic activity.

The failure of the dehydrated samples was likely due to a combination of human and chemical error. During the first drying step, the vacuum pump was turned off *after* the spinning rotor was stopped. This resulted in significant bumping and solid reagent loss. It is unclear precisely how much solid was lost, and from which samples this solid was ejected. However, it is possible that this loss may have affected some of the samples more than others, leading to dead runs that lacked one or more of the essential reagents. Regarding chemical difficulties, EDTA was added to each dehydrated sample after the addition of zirconium and subsequent precipitation of white solid (which was likely zirconium phosphate). While EDTA would have exchanged zirconium with this precipitate to some extent, the rate may not have been high enough to generate sufficient levels of zirconium-EDTA catalyst. Had the zirconium first been incubated with EDTA, this exchange issue would have been avoided, and the ion's catalytic activity could have been more thoroughly preserved.

It is also possible that products of the dehydrated samples were not UV-active. Over the 5-day heating interval, many of the dehydrated samples turned gold in color (DS 6, DS 8, and DS 9). Despite this color change, no observable changes were observed on any of the TLCs, even with the use of two different solvent systems. In chemistry, a color change is almost always indicative of a chemical reaction. In this case, we can be sure that the species producing the color change is not benzyl phosphate since aromatic rings usually absorb UV light (benzyl phosphate is also a colorless compound). However, the color change may still be indicative of other interesting chemistry, and a method of deeper inquiry like mass spectrometry would be needed to confirm the chemical composition of these gold samples.

The TE samples were the final set of conditions tested and showed the most promising results with the demonstration of clear polar spots. While these spots were located within two of the control lanes, it should be noted that the same spatula was used to mix each of the TE samples before heating. This spatula was wiped dry between each mixing but *not* rinsed. This means it is possible that zirconium or phosphate found their way into the respective controls and instigated reactions within these Eppendorf tubes.

Because of the potential success of the TE samples, many of the methods used to generate these samples will be replicated or at the very least adapted for future trials. For example, future runs will incubate zirconium with EDTA or Tris for a few hours before the addition of phosphate buffer. This will minimize or eliminate the formation of zirconium phosphate derivatives through the alternative formation of metal organic frameworks (MOFs), whereby zirconium is chelated by these ligands (Nabi et al. 2009). Because EDTA is known to partially quench the reactivity of zirconium (Ott and Krämer 1998), Tris would be the preferable ligand for this kind of MOF formation. Tris has also been previously shown to hydrolyze RNA or DNA fragments in MOFs containing zirconium. These frameworks have hydrolytic capacity in conjunction with peptide nucleic acids (Zelder et al. 2003) and under weakly acidic conditions ranging from pH 4-5 (Ott

and Krämer 1999). Because of Tris's extensive ability to catalyze hydrolysis reactions, it seems feasible to use this ligand as the starting point for any future nucleoside phosphorylation reactions. Additionally, the TE trials will be reproduced in the future with special emphasis placed on contamination avoidance. Samples exclusively containing the Tris ligand will also be prepared to see if different combinations of chelators affect the favorability of phosphate formation reactions.

Numerous other routes are also worth investigating. While individual cerium (IV) ions and heterogeneous cerium complexes have been shown to be prone to reduction to Ce^{3+}, they remain some of the best metal species for DNA hydrolysis (Ott and Krämer 1999, Sreedhara and Cowan 2001). As such, it might be beneficial to test a variety of different cerium-based samples for their ability to catalyze phosphate bond chemistry. Alternatively, new metal ions or frameworks may be better suited to phosphomonoester or phosphodiester formation. Europium (III) salt solutions and complexes containing cobalt (III) have historically shown semi-catalytic activity (these complexes accelerate the reaction but have poor turnover) in DNA or RNA hydrolysis (Ott and Krämer 1999). While the kinetic rates of these metal ions are inferior to zirconium (about 20-fold lower), side reactions like the formation of zirconium phosphate might be limited (Ott and Krämer 1999). In turn, these complexes might provide more practical explanations for RNA formation during Earth's early days. Ultimately, the many avenues described above provide an array of new opportunities to unravel the mysteries surrounding the origins of our biological planet.

References

13.10: Phosphoester Formation. (2014, August 20). Chemistry LibreTexts. https://chem.libretexts.org/Courses/Sacramento_City_College/SCC%3A_Chem_309_-_General_Organic_and_Biochemistry_(Bennett)/Text/13%3A_Functional_Group_Reactions/13.10%3A_Phosphoester_Formation

14.7: Catalysis. (2015, February 6). Chemistry LibreTexts. https://chem.libretexts.org/Bookshelves/General_Chemistry/Map%3A_Chemistry_-_The_Central_Science_(Brown_et_al.)/14%3A_Chemical_Kinetics/14.7%3A_Catalysis

Alberts, B., Johnson, A., Lewis, J., Raff, M., Roberts, K., & Walter, P. (2002). The RNA World and the Origins of Life. Molecular Biology of the Cell. 4th Edition. https://www.ncbi.nlm.nih.gov/books/NBK26876/

Awual, M., Jyo, A., Ihara, T., Seko, N., Tamada, M., & Lim, K. T. (2011). Enhanced trace phosphate removal from water by zirconium(IV) loaded fibrous adsorbent. Water Research, 45(15), 4592–4600. https://doi.org/10.1016/j.watres.2011.06.009

Berkessel, A., & Herault, D. (1999, January 15). Discovery of Peptide–Zirconium Complexes That Mediate Phosphate Hydrolysis by Batch Screening of a Combinatorial Undecapeptide Library. https://onlinelibrary.wiley.com/doi/epdf/10.1002/%28SICI%291521-3773%2819990115%2938%3A1/2%3C102%3A%3AAID-ANIE102%3E3.0.CO%3B2-H

Hevesy, G., & Kimura, K. (2002, May 1). THE SOLUBILITIES OF THE PHOSPHATES OF ZIRCONIUM AND HAFNIUM (world). ACS Publications; American Chemical Society. https://doi.org/10.1021/ja01687a016

Lunine, J. I. (2006). Physical conditions on the early Earth. Philosophical Transactions of the Royal Society B: Biological Sciences, 361(1474), 1721. https://doi.org/10.1098/rstb.2006.1900

Nabi, S. A., Naushad, M., & Bushra, R. (2009). A New Hybrid EDTA–Zirconium Phosphate Cation-Exchanger: Synthesis, Characterization and Adsorption Behaviour for Environmental Monitoring: Adsorption Science & Technology. https://doi.org/10.1260/026361709790252641

Ott, R., & Krämer, R. (1998). Rapid Phosphodiester Hydrolysis by Zirconium(IV). Angewandte Chemie International Edition, 37(13–14), 1957–1960. https://doi.org/10.1002/(SICI)1521-3773(19980803)37:13/14<1957::AID-ANIE1957>3.0.CO;2-0

Ott, R., & Krämer, R. (1999, May 28). DNA hydrolysis by inorganic catalysts—ProQuest. https://www.proquest.com/docview/884649630

Salván, C., Bouza, M., Fialho, D., Burcar, B., Fernández, F., & Hud, N. (2020). Prebiotic Origin of Pre-RNA Building Blocks in a Urea "Warm Little Pond" Scenario. Chembiochem : A European Journal of Chemical Biology, 21(24). https://doi.org/10.1002/cbic.202000510

Sreedhara, A., & Cowan, J. A. (2001). Catalytic hydrolysis of DNA by metal ions and complexes. Journal of Biological Inorganic Chemistry : JBIC : A Publication of the Society of Biological Inorganic Chemistry, 6(4). https://doi.org/10.1007/s007750100209

Thin Layer Chromatography. (n.d.). Retrieved March 17, 2022, from https://www.sigmaaldrich.com/US/en/applications/analytical-chemistry/thin-layer-chromatography#TLC-Retention-Factor

Thin Layer Chromatography. (2013, October 2). Chemistry LibreTexts. https://chem.libretexts.org/Ancillary_Materials/Demos_Techniques_and_Experiments/General_Lab_Techniques/Thin_Layer_Chromatography

Thin Layer Chromatography (TLC). (n.d.). Retrieved March 23, 2022, from https://www.orgchemboulder.com/Technique/Procedures/TLC/TLC.shtml

Trefil, J., Morowitz, H., & Smith, E. (2017, February 6). The Origin of Life. American Scientist. https://www.americanscientist.org/article/the-origin-of-life

Yang, L., Arora, K., Beard, W., Wilson, S., & Schlick, T. (2004). Critical role of magnesium ions in DNA polymerase beta's closing and active site assembly. Journal of the American Chemical Society, 126(27). https://doi.org/10.1021/ja049412o

Zelder, F., Mokhir, A., & Krämer, R. (2003, November 20). Sequence Selective Hydrolysis of Linear DNA Using Conjugates of Zr(IV) Complexes and Peptide Nucleic Acids (world) [Rapid-communication]. ACS Publications; American Chemical Society. https://doi.org/10.1021/ic034896v

Zhou, Y.-H., Zhang, Z., Patrick, M., Yang, F., Wei, R., Cheng, Y., & Gu, J. (2019). Cleaving DNA-model phosphodiester with Lewis acid–base catalytic sites in bifunctional Zr–MOFs. Dalton Transactions, 48(23), 8044–8048. https://doi.org/10.1039/C9DT00246D